CHIN. PHYS. LETT. Vol. 26, No. 1 (2009) 016102

Pressure-Induced Phase Transition of Ruthenium Diboride *

REN Feng-Zhu(任凤竹), WANG Yuan-Xu(王渊旭)**, ZHANG Guang-Biao(张光彪)

Institute of Computational Materials Science, School of Physics and Electronics, Henan University, Kaifeng 475004

(Received 10 September 2008)

Based on the first-principles calculations, we firstly predict that RuB_2 undergoes a phase transition from the orthorhombic phase to the hexagonal phase with a volume collapse of 1% when the applied pressure is 15.7 GPa. The values of calculated elastic moduli indicate that RuB_2 and RuN_2 are low compressibility materials. Based on the calculated electronic density of states and valence charge density distribution, the bonding nature of RuB_2 is examined to obtain a deeper insight into the physical origin of the mechanical properties. The metallicity and high elastic moduli of RuB_2 and RuN_2 suggest that they are potential hard conductors.

PACS: 61. 50. Ks, 71. 15. Mb, 71. 20. −b, 62. 20. Dc, 64. 60. −i

With superior properties of higher compressional strength, thermal conductivity, refractive index, and chemical stability besides higher hardness, hard materials have been widely used in industry. Therefore, to design and to explore superhard or hard materials will naturally be a research subject of permanent interest due to their importance in both fundamental science and technique applications. One of the strategies employed for the development of hard or superhard materials is offered by incorporating light elements into heavy transition metals to optimize covalent bonding and valence-electron density. Therefore, transition-metal (TM) boride, carbide, nitride, or oxide may be the most interesting candidates as hard materials. Five compounds PtN_2, IrN_2, OsN_2, OsB_2, and ReB_2 with a bulk modulus above 350 GPa have been synthesized under high pressure or at high temperature, respectively.[1−5] Because these high bulk modulus compounds are synthesized under high pressure, it is very interesting to explore whether the pressure-induced phase transition exists. For example, Chen *et al.* noted that the pressure-induced phase transition for OsB_2 occurs at 2.5 GPa.[6] RuB_2 was synthesized and was reported to be an ultra-incompressible material.[7] Recently, Chiodo *et al.*[8] investigated its mechanical properties and electronic properties. Wang *et al.*[9] studied the lattice dynamics and superconductivity of RuB_2. However, there is no report on the pressure-induced phase transition to our best knowledge. In this Letter, we study the possibility of the pressure-induced phase transition for RuB_2 for the first time.

We employ the projector-augmented wave (PAW) method within the density functional theory as implemented in the Vienna *ab initio* simulation program (VASP).[10] The generalized gradient approximation[11] (GGA) and the local density approximation[12] (LDA) are both used with the PAW potential. For RuB_2, we consider three structures: OsB_2-type structure (space group $Pmmn$), ReB_2-type structure (space group $P6_3/mmc$), AlB_2-type structure (space group $P6/mmm$). Marcasite (space group $Pnnm$) and Pyrite (space group $Pa3$) structures are used for RuN_2 as inputs for the calculations. The cutoff energy is 500 eV. The Monkhorst-Pack grids of $11 \times 15 \times 12$ for OsB_2-type RuB_2, $14 \times 14 \times 10$ for ReB_2-type RuB_2, $14 \times 14 \times 10$ for AlB_2-type RuB_2, $11 \times 10 \times 14$ for macarsite RuN_2, and $17 \times 17 \times 17$ for pyrite RuN_2 are used.[13] The structures are fully relaxed with the conjugate-gradient algorithm method. The optimized cell volume for OsB_2-type RuB_2 is very close to the experimental value (53.83 Å^3 [14,15]).

Table 1. Calculated lattice constants (Å), equilibrium cell volume V(Å^3), relative total energy ΔE_0(eV), bulk modulus B(GPa), and its pressure derivative at zero pressure B_1 for RuB_2 and RuN_2.

Type	V_0	ΔE_0	B	B_1
OsB_2-type (LDA)	52.53	0	315	4.21
OsB_2-type (GGA)	54.62	0	283	4.39
ReB_2-type (LDA)	52.04	0.015	321	4.16
ReB_2-type (GGA)	52.07	0.049	292	4.14
AlB_2-type (LDA)	50.04	2.667	327	4.12
AlB_2-type (GGA)	52.20	2.546	289	4.37

Table 1 lists the calculated equilibrium volume, relative total energy, the bulk modulus, and the pressure derivative of the bulk modulus for RuB_2. The bulk modulus and its pressure derivative are obtained by fitting the calculated pressure at each volume to the third-order Birch-Murnaghan equation of state.[16] As seen in Table 1, the energy of the OsB_2-type RuB_2 is lower than that of the ReB_2-type at zero pressure, which implies that the OsB_2-type RuB_2 is more stable than ReB_2-type. Since the two structures are so close in energy, i.e., the ReB_2-type phase is only 0.049 eV

*Supported by the Programme for Science and Technology Innovation Talents in Universities of Henan Province under Grant No 2009HASTIT003, the Natural Science Foundation of Henan University under Gant Nos 07ZRZD005 and 07YBZR046, and the Foundation of Science and Technology Department of Henan Province under Grant No 082300410010.

**To whom correspondence should be addressed. Email: wangyx@henu.edu.cn

© 2009 Chinese Physical Society and IOP Publishing Ltd

(GGA) higher in energy than the OsB_2-type one, a phase transition is expected to take place under pressure. To determine the transition pressure, only the enthalpy ($H = E_{\text{energy}} + PV$) should be considered. For a given pressure, a stable structure is the one for which the enthalpy has the lowest value. Hence, the common tangent of the intersection in enthalpy-pressure curves indicates the phase transition pressure. We display the relative enthalpy as a function of pressure with respect to the ReB_2-type phase in Fig. 1(a). Our calculated phase transition pressure is estimated to be 15.7 GPa. In addition, the relationship between pressure and volume for two phases are shown in Fig. 1(b). It is clear to see that during the structural phase transition, the calculated value of the volume collapse of 1% which is accompanied with the structural phase transition, but the calculated value of the volume collapse still required further experimental identification.

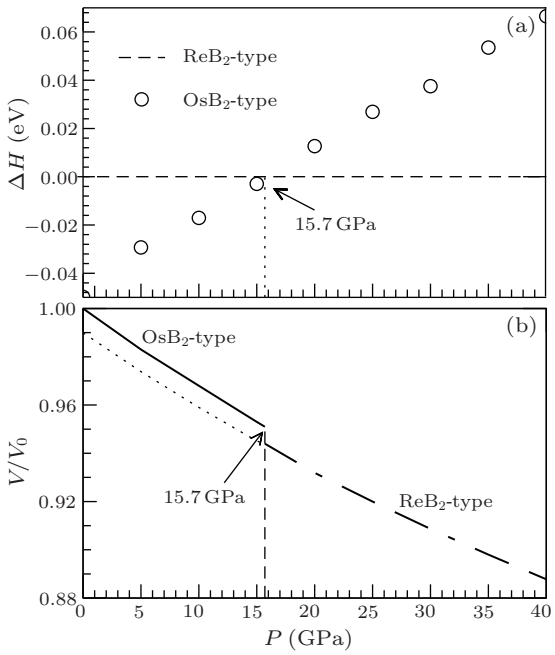

Fig. 1. (a) Relative enthalpy of RuB_2 in the ReB_2-type and OsB_2-type phases as a function of pressure with GGA; (b) relationship between pressure and volume for the ReB_2-type and OsB_2-type phases of RuB_2.

The calculated elastic constants of RuB_2 and RuN_2 are summarized in Table 2. The bulk modulus B and the shear modulus G in this table are calculated by the Voigt–Reuss–Hill approximation method.[17] Young's modulus E and Poisson's ratio υ are calculated by $E = 9BG/(3B + G)$ and $\upsilon = (3B - 2G)/[2(3B + G)]$. We also calculate the eigenvalues of the elastic constant matrix and find that RuB_2 with the considered three type structures are all elastically stable. Hao *et al.*[18] calculated the elastic constants of orthorhombic RuB_2 by the first-principles method. Their reported bulk modulus (290 GPa) and shear modulus (184 GPa) are very similar to our results listed in Table 2. Pyrite RuN_2 is found to be unstable under the ambient condition.

Hardness is a macroscopic concept. The bulk and shear moduli are the most important parameters indirectly governing the hardness. It can be seen in Table 2 that our calculated bulk modulus agrees with that derived from the third-order Birch-Murnaghan equation of state. We find unusually high incompressibilities along the c-axis in the ReB_2-type RuB_2, as demonstrated by the large C_{33} value (in Table 2). It is interesting to notice that the ReB_2-type RuB_2 has higher bulk and shear moduli than the OsB_2-type one at zero pressure. From Table 1, it can be found that the optimized cell volume of the ReB_2-type structure is smaller than that of the OsB_2-type one, which partially contributes the higher bulk and shear moduli of the ReB_2-type structure. In addition to the reason mentioned above, the elastic constants C_{12}, C_{13}, and C_{33} are also responsible for the higher bulk and shear moduli of the ReB_2-type structure than the OsB_2-type one. Also, it is interesting to note that the C_{33} value of the OsB_2-type structure are only slightly lower than that of the ReB_2-type one. By comparison, the elastic constants (C_{11} and C_{22}) for deformation along the a and b axes in RuB_2 are about 200–400 GPa lower than its C_{33} counterparts. For RuB_2, the C_{33} value of the AlB_2-type structure is about half of the OsB_2-type and ReB_2-type ones. For marcasite RuN_2, the high incompressibility along the a and b axes may come from the large elastic constants C_{11} and C_{22}. In general, the elastic moduli of 4d TM compounds are smaller than that of 5d TM compounds, such as $G_{TcB_2} < G_{ReB_2}$ [19] and $G_{RuN_2} < G_{OsN_2}$,[20] while our calculated shear modulus for RuB_2 (188 GPa) is higher than that of OsB_2 (168 GPa).[21] The high shear modulus of RuB_2 partially results from its larger C_{44} (108 GPa) as compared with that of OsB_2[21] (60 GPa). The large elastic constant C_{44} means a strong ability of resisting the monoclinic shear distortion in (100) plane.

Table 2. Calculated elastic constants (GPa), bulk modulus B(GPa), shear modulus G(GPa), Young's modulus E(GPa), Poisson's ratio υ, and G/B for RuB_2, and RuN_2.

	C_{11}	C_{12}	C_{13}	C_{22}	C_{23}	C_{33}	C_{44}	C_{55}	C_{66}	B	G	E	υ	G/B
RuB_2 (OsB_2-type)	516	187	156	456	125	698	108	217	176	287	188	463	0.23	0.66
RuB_2(ReB_2-type)	452	191	169			819	204		131	309	203	500	0.23	0.66
RuB_2(AlB_2-type)	450	262	194			429	21		94	291	58	163	0.41	0.20
RuN_2(Marcasite)	595	147	213	740	79	432	94	262	112	288	190	467	0.23	0.66

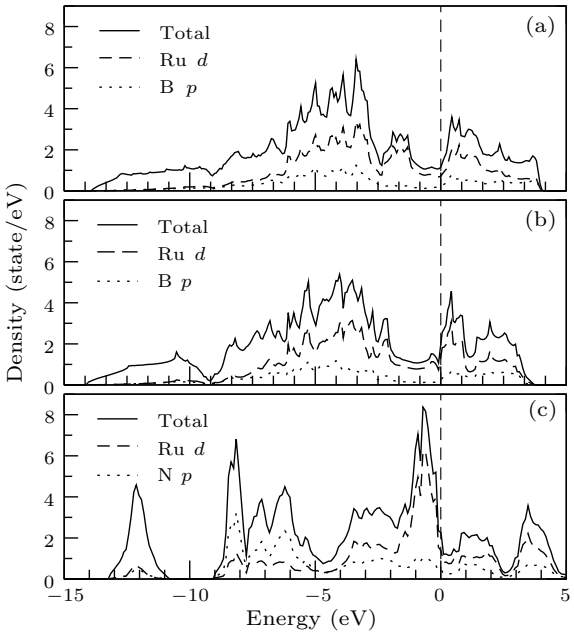

Fig. 2. Total and partial DOS with GGA: (a) OsB_2-type structure for RuB_2, (b) ReB_2-type structure for RuB_2, (c) Marcasite structure for RuN_2. The dashed line represents the Fermi surface.

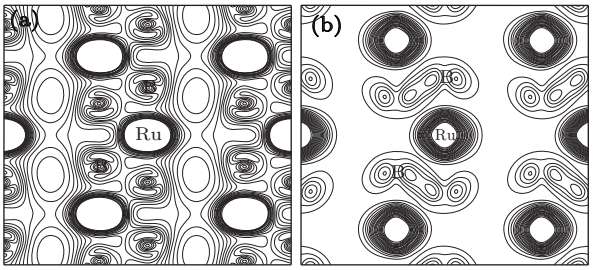

Fig. 3. Valence charge density contour (e/a.u.^{3}) distribution in (110) plane for the ReB_2-type RuB_2. (a) Occupied charge density in the energy range of −10.0–0.0 eV. (b) Unoccupied charge density in the energy range of 0.0–3.0 eV. The values of the contours in the figure are from 0.0 to 0.9 e/a.u.^{3} with an increment of 0.05 e/a.u.^{3}.

In order to elucidate the origin of the mechanical properties for RuB_2 and RuN_2, the electronic density of state (DOS) and charge density are calculated. As seen in Fig. 2, the existence of electrons near Fermi level E_f implies the metallicity of RuB_2 and RuN_2. The typical feature of the total DOS of these compounds is the presence of a deep valley at E_f and this valley is referred to as a pseudogap. The presence of pseudogap indicates the existence of covalent bonding in these compounds. There exists a correlation between structural stability and the position of E_f with respect to the pseudogap. We observe that E_f lies on the pseudogap in RuB_2 and RuN_2, which indicates that these compounds are all stable. In order to make sense of the bonding properties, the valence charge density distribution of the ReB_2-type RuB_2 in (110) plane corresponding to occupied and unoccupied bands are shown in Figs. 3(a) and 3(b), respectively. The interesting aspect of Fig. 3(a) is that some electrons around the B atoms are deviation toward the nearest Ru atoms, indicating a strong directional covalent Ru–B bonding. Furthermore two neighbouring boron atoms also form a strong covalent bond. It is emphasized that the formation of these directional covalent bonds partially increases their hardness.

In summary, the possible pressure-induced phase transition of RuB_2 has been investigated. It is theoretically predicted that the calculated phase transition point from OsB_2-type phase to ReB_2-type phase is at about 15.7 GPa. The computed bulk moduli indicate that they are potential low compressible materials. The strong directional covalent bonds and relatively high shear modulus suggest that RuB_2 and RuN_2 are also hard materials. RuB_2 and RuN_2 are found to be metallic. Therefore, RuB_2 and RuN_2 are important for the potential technological and industrial applications. We hope that our calculations will further stimulate experimental research on these compounds.

References

[1] Gregoryanz E, Sanoup C, Somayazulu M, Badro J, Fiquet G, Mao H K and Hemley R J 2004 *Nat. Mater.* **3** 294
[2] Crowhurst J C, Goncharov A F, Sadigh B, Evans C L, Morrall P G, Ferreira J L and Nelson A J 2006 *Science* **311** 1275
[3] Young A F, Sanloup C, Gregoryanz E, Scandolo S, Hemley R J and Mao H K 2006 *Phys. Rev. Lett.* **96** 155501
[4] Cumberland R W, Weinberger M B, Gilman J J, Clark S M, Tolberks S H and Kamer R B 2005 *J. Am. Chem. Soc.* **127** 7264
[5] Chung H Y, Weinberger M B, Levine J B, Kavner A, Yang J M, Tolbert S H and Kaner R B 2007 *Science* **316** 436
[6] Chen X Q, Fu C L, Krčmar M and Painter G S 2008 *Phys. Rev. Lett.* **100** 196403
[7] Chung H Y, Weinberger M B, Levine J B, Kavner A, Yang J M, Tolbert S H and Kaner R B 2008 *Appl. Phys. Lett.* **92** 261904
[8] Chiodo S, Gotsis H J, Russo Nand Sicilla E 2006 *Chem. Phys. Lett.* **425** 311
[9] Wang Y Q, Yuan L F and Yang J L 2008 *Chin. Phys. Lett.* **25** 3036
[10] Kresse G and Hafner J 1993 *Phys. Rev.* B **47** R558
[11] Perdew J P, Burke K and Ernzerhof M 1996 *Phys. Rev. Lett.* **77** 3865
[12] Ceperley D. M. and Alder B. J. 1980 *Phys. Rev. Lett.* **45** 566
[13] Pack J D and Monkhorst H J 1977 *Phys. Rev. B* **16** 1748
[14] Aronsson B 1963 *Acta Chem. Scand.* **17** 2036
[15] Gu Q F, Krauss G and Steurer W 2008 *Adv. Mater.* **20** 3620
[16] Birch F 1947 *Phys. Rev.* **71** 809
[17] Hill R 1980 *Proc. Phys. Soc. London* **45** 566
[18] Hao X F, Xu Y H, Wu Z J, Zhou D F, Liu X J and Meng J 2008 *J. Alloys. Compd.* **453** 413
[19] Wang Y X 2007 *Appl. Phys. Lett.* **91** 101904
[20] Wang Y X, Arai M and Sasaki T 2007 *Appl. Phys. Lett.* **90** 061922
[21] Gou H Y, Hou L, Zhang J W, Li H, Sun G F and Gao F M 2006 *Appl. Phys. Lett.* **88** 221904